Title

Voice production in a MRI-based subject-specific vocal fold model with parametrically controlled medial surface shape

Journal

The Journal of the Acoustical Society of America, 146(6)

ISSN

0001-4966

Authors

Wu, Liang
Zhang, Zhaoyan

Publication Date

2019-12-01

DOI

10.1121/1.5134784

Peer reviewed

Voice production in a MRI-based subject-specific vocal fold model with parametrically controlled medial surface shape

Liang Wu and Zhaoyan Zhang[a)]
Department of Head and Neck Surgery, University of California, Los Angeles (UCLA), 31-24 Rehabilitation Center, 1000 Veteran Avenue, Los Angeles, California 90095-1794, USA

(Received 5 August 2019; revised 24 October 2019; accepted 30 October 2019; published online 9 December 2019)

The goal of this study was to investigate how realistic changes in medial surface shape, as occur in human phonation, affect voice production. In a parametric magnetic resonance imaging-based three-dimensional vocal fold model, the superior and inferior portions of the medial surface were systematically manipulated to produce different medial surface contours similar to those observed in previous excised larynx and *in vivo* canine larynx experiments. Voice simulations were performed to investigate the differences in the resulting voice production. The results showed that both superior-medial bulging and inferior-medial bulging of the medial surface, which led to an increased vertical thickness and a more rectangular glottal configuration, increased the closed quotient of vocal fold vibration. Changes in medial surface shape also had significant effects on the phonation threshold pressure. The degree of these effects of changes in medial surface shape was larynx specific, and varied significantly depending on the vocal fold cross-sectional geometry and its variation along the anterior-posterior direction. The results suggest that, in addition to vocal fold approximation, surgical interventions of voice disorders should also aim at restoring a rectangular and sufficiently thick medial surface. © *2019 Acoustical Society of America*.
https://doi.org/10.1121/1.5134784

[JFL] Pages: 4190–4198

I. INTRODUCTION

Voice production involves a complex interaction between the vocal folds and glottal airflow (Zhang, 2016a). Because this complex fluid–structure interaction occurs primarily on the medial surface of the vocal folds, the medial surface shape has long been considered to play an important role in voice production (Sundberg and Högset, 2001; Scherer *et al.*, 2001; Berry *et al.*, 2001; Thomson *et al.*, 2005; Döllinger *et al.*, 2005; Pickup and Thomson, 2011; Zhang, 2016b). While there have been attempts to investigate the effect of medial surface shape on phonation in *in vivo* or excised larynx models (Mau *et al.*, 2012; Chhetri *et al.*, 2012; Chhetri *et al.*, 2014), systematic investigation is difficult due to the challenges of direct visualization and the fact that changes in medial surface shape in these models are often accompanied by changes in vocal fold approximation and stiffness. As a result, computational or physical models are often used to study the effect of medial surface shape (e.g., Titze and Talkin, 1979; Chan *et al.*, 1997; Lucero, 1998; Alipour and Scherer, 2000; Zhang, 2008, 2016b). These studies showed that the phonation threshold pressure is the lowest for a rectangular or near-rectangular medial surface, and increases significantly when the medial surface becomes either convergent or divergent (Chan *et al.*, 1997; Lucero, 1998; Zhang, 2008). Changes in medial surface vertical thickness also play an important role in regulating the closure pattern of vocal fold vibration with thicker folds generally exhibiting longer periods of glottal closure during phonation and stronger excitation of higher-order harmonics in the voice spectra (Zhang, 2016b).

While these studies have provided important insight, direct translation of their findings to human phonation is not always straightforward due to the simplified vocal fold geometry used in these studies. Often, the cross-sectional geometry is simplified so that it can be controlled by a few parameters. For example, Fig. 1 compares the coronal cross section of the simplified vocal fold model used in Zhang (2017) with coronal contours of realistic human vocal folds. While the simplified geometry in Fig. 1(a) has a well-defined medial surface (region of considerable constriction of the glottal channel), realistic vocal fold contours often do not have a well-defined medial surface, and thus it is difficult to calculate an effective vertical thickness. The medial surface curvature also changes continuously and cannot be quantified by a single convergent angle as in simplified geometries. In humans, medial surface shape also varies under laryngeal muscle activation. Figure 1(c) shows the coronal cross sections of an excised human larynx at rest and under simulated lateral cricoarytenoid (LCA) muscle activation. Figure 1(d) further shows the movement of the medial surface contour in a canine larynx under individual and combined stimulations of the LCA and thyroarytenoid (TA) muscles (Vahabzadeh-Hagh *et al.*, 2017).

Titze and Talkin (1979) modeled changes in medial surface shape due to activation of the TA muscle by introducing a bulging factor in their simplified vocal fold geometry that allowed the middle portion of the medial surface to bulge toward the glottal midline. They showed that inferior medial bulging increased vocal efficiency. Using a similar geometry,

[a)]Electronic mail: zyzhang@ucla.edu

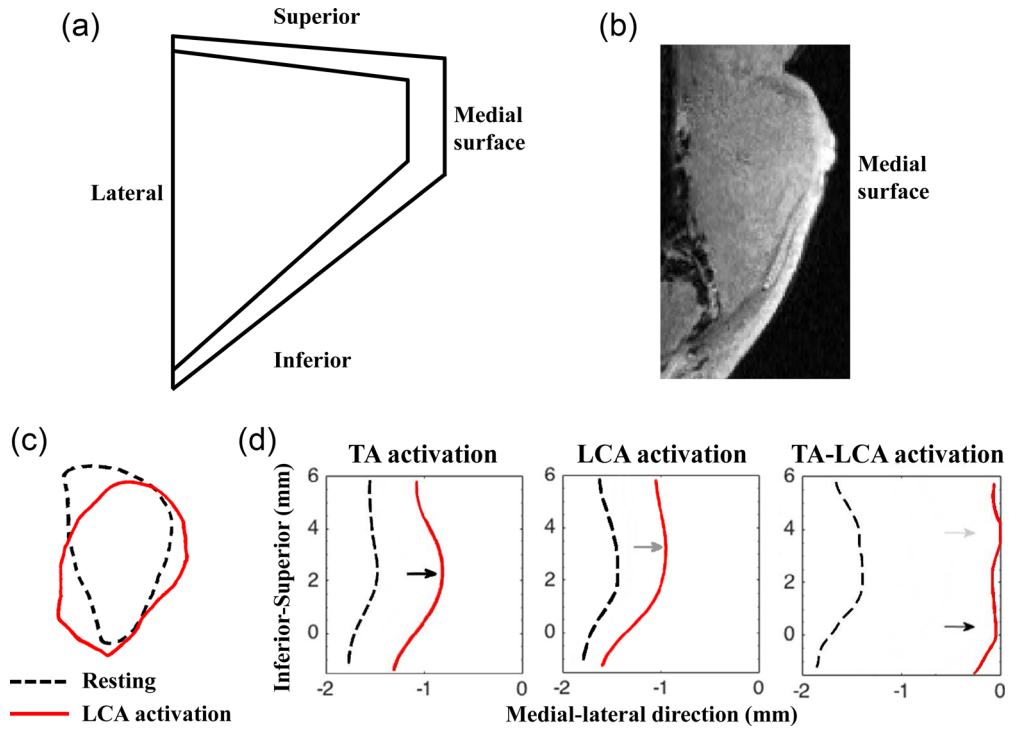

FIG. 1. (Color online) Comparison between coronal cross sections of (a) the simplified vocal fold geometry used in Zhang (2017) and (b) a realistic human vocal fold. (c) shows the MRI-reconstructed coronal cross-sectional contour of a human excised larynx at rest (black dashed line) and under simulated lateral cricoarytenoid (LCA) muscle activation (red solid line). (d) shows changes in the medial surface contour in an *in vivo* canine larynx due to activation of the thyroarytenoid (TA), LCA, and combined TA-LCA activation (adapted from Fig. 6 in Vahabzadeh-Hagh *et al.*, 2017). The black and gray arrows show the positions of the medial bulging induced by the TA and LCA muscle activation, respectively.

Alipour and Scherer (2000) showed that medial bulging increased glottal flow resistance and decreased the maximum glottal opening and mean glottal volume velocity. However, the effect of medial bulging on the closure pattern of vocal fold vibration was not investigated in these studies.

In addition to difference in cross-sectional geometry, human vocal folds also exhibit geometric variation along the longitudinal direction in thickness and width (Wu and Zhang, 2016), which is often neglected in computational models. An example of such inter-larynx differences in cross-sectional shape, and its longitudinal variation is given in Fig. 2, which shows laryngeal geometry of two excised human larynges obtained from magnetic resonance imaging (MRI).

Thus, there is a need to develop a vocal fold model capable of reproducing realistic medial surface contours as observed in human phonation [e.g., those shown in Figs. 1(c) and 1(d)] and investigate how different realistic medial surface shapes affect voice production. For example, would changes in realistic medial surface shape as shown in Figs. 1(c) and 1(d) have the same effect on the phonation threshold pressure and glottal closure pattern as observed in previous studies using simplified geometry? How would longitudinal variation in medial surface shape affect voice production? Answers to these questions are particularly important to clinical intervention of voice disorders. Currently, surgical intervention (e.g., medialization laryngoplasty) often focuses on reducing the glottal gap from a superior view, and the medial surface shape has received little attention. If changes in medial surface shape as shown in Figs. 1(c) and 1(d) have a large effect on the closure pattern of vocal fold vibration and output voice spectra as shown in previous studies using simplified vocal fold geometry, it would suggest that surgical intervention of voice disorders should also consider the effect of the intervention on medial surface shape.

Toward this goal, we used a parametric MRI-based vocal fold model which allowed realistic three-dimensional larynx-specific vocal fold geometry (Wu and Zhang, 2016). While changes in medial surface shape due to laryngeal muscle activation can be directly modeled (e.g., Yin and Zhang, 2016), such an approach requires detailed data of laryngeal geometry and mechanical properties and is computationally expensive. In this study, we took a different approach by developing an empirically based two-step control scheme, based on previous *in vivo* and excised larynx experiments, to directly manipulate the superior and inferior portion of the medial surface to produce medial surface shapes similar to those in Figs. 1(c) and 1(d). In the following, the details of the models, simulations, and data analysis are described in Sec. II. The effects of the changes in medial surface shape on phonation are then presented in Sec. III, followed by discussion in Sec. IV.

II. METHODS

A. MRI-based parametric vocal fold model

Two human larynges (a 57-year-old male L1 and a 28-year-old male L2) were harvested from autopsy and were used in MRI scanning. The three-dimensional laryngeal geometry,

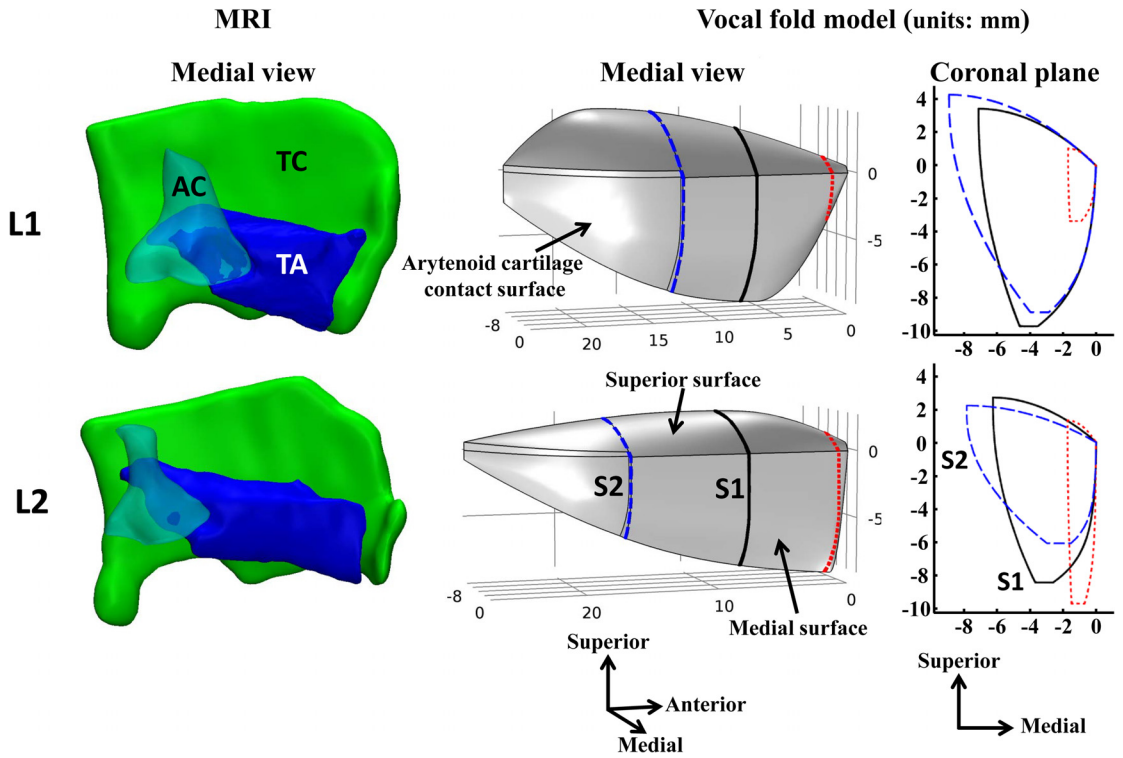

FIG. 2. (Color online) (Left) MRI-reconstructed resting geometry of the thyroid cartilage (TC, green), arytenoid cartilage (AC, semi-transparent light blue), and vocal fold (TA, blue) of larynx L1 (top) and L2 (bottom). (Middle) Parametric vocal fold models derived from the MRI reconstructions. (Right) Cross-sectional contours of the vocal folds at three longitudinal locations as indicated in the middle panel. The two cross-sections S1 (solid black line) and S2 (dashed blue line) in larynx L2 were used to develop two section models as described in Sec. III B.

including the lamina propria, the TA muscle or vocal fold body, other laryngeal muscles, and cartilages were segmented and reconstructed from the MRI images. A parametric vocal fold model was developed for each larynx as described in Wu and Zhang (2016). Compared with the three-dimensional MRI reconstruction, this parametric model is defined based on anatomical landmarks, such as the length, thickness, and width of the vocal folds, and thus allows easy adaptation to subject-specific geometry. More importantly, the analytical formulation of the model allows systematic manipulation of the medial surface shape as described below in Sec. II B, which otherwise is not possible if the MRI-reconstructed geometry were used. Figure 2 shows the three-dimensional geometries and the corresponding parametric vocal fold models for the two larynges. Notable differences can be observed between the two larynges. Compared with larynx L1, larynx L2 was much longer in the anterior-posterior (AP) direction and slightly thinner in the superior-inferior direction (except close to the anterior edge at which the medial surface was thicker in L2).

Note that Wu and Zhang (2016) used a second-degree polynomial function to describe the resting medial surface contour. As the present study focused on the medial surface shape, we re-evaluated the goodness of fit and found out that the second-degree polynomial function did not sufficiently approximate the curvatures of the medial surface contour. Instead of using higher degree polynomial functions, in this study, the cross-sectional contours of the medial surface at the resting position were described by a sigmoid function, which was found to better curve fit the resting medial surface contour.

B. Control of medial surface shape

The parametric vocal fold models in Fig. 2 were derived from cadaver excised larynges, and thus represented vocal fold geometry at the resting position. During phonation, vocal fold posturing would change vocal fold geometry, including length, width, medial surface contour, etc., and vocal fold stiffness. In this study, in order to focus on the effect of changes in medial surface shape, we assumed the medial edge of the vocal folds were positioned at the glottal midline and kept other geometric features and stiffness unchanged as the medial surface shape was manipulated.

Previous studies using excised human larynges (Hirano, 1988) and *in vivo* canine models (Vahabzadeh-Hagh *et al.*, 2017) showed that activation of the TA muscle often causes the inferior portion of the medial surface to bulge more toward the glottal midline [Fig. 1(d)], whereas activation of the LCA muscle causes the superior portion of the medial surface to bulge toward the glottal midline. In combination, activation of the TA and LCA muscles often leads to a more rectangular medial surface. The superior-medial bulging effect of the LCA muscle was also observed in our recent MRI study of vocal fold deformation due to simulated LCA muscle activation [Fig. 1(c)].

Based on these observations, in this study, the medial surface was manipulated in two steps, corresponding to superior-medial bulging and inferior-medial bulging, as shown in Fig. 3. The superior-medial bulging was achieved by superimposing on the resting medial surface an exponentially damped sinusoidal function,

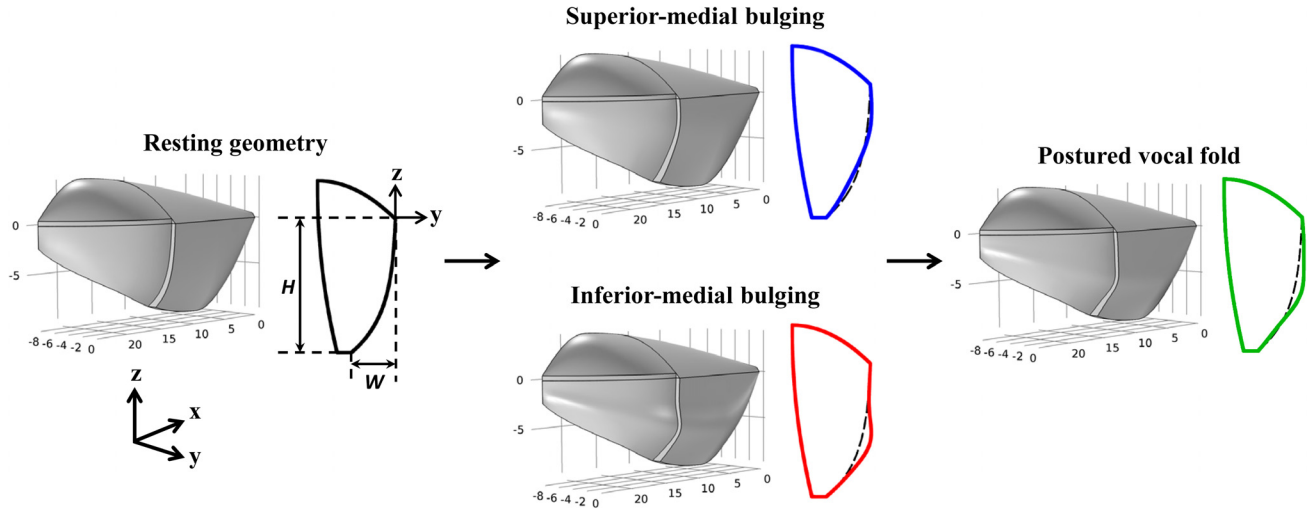

FIG. 3. (Color online) Two-step manipulation of the medial surface contour through superior and inferior medial bulging. Superior medial bulging simulates a medial and downward rotation motion of the medial surface due to LCA muscle activation, whereas inferior medial bulging simulates the effect of TA muscle activation. Each panel shows the three-dimensional vocal fold model and the mid-membranous cross-section contour. In the left panel, cross sectional height H and width W of the vocal fold were used as normalization references in Eqs. (1) and (2). In the three panels on the right, the dashed lines represent the resting medial surface contour.

$$\frac{y_s}{W} = \alpha_s A1 \exp\left(k\frac{z}{H}\right)\sin\left(-2\pi\frac{z}{H}\right), \quad z \in [-H, 0], \tag{1}$$

where H and W are the height and width of the vocal fold cross sections (Fig. 3), respectively, $A1$ and k are model coefficients controlling maximum superior medial bulging $A_{\max,s}$ and the vertical location $z_{\max,s}$ at which the maximum bulging occurs, respectively, and α_s is a scale factor that ranges between 0 and 1. This function form was chosen because of its capability to curve fit changes in medial surface contour as shown in Fig. 1(c). The inferior-medial bulging was achieved by superimposing a Gaussian-damped sinusoidal function (Vahabzadeh-Hagh *et al.*, 2017),

$$\frac{y_i}{W} = \alpha_i A2 \exp\left(-\frac{\left(\frac{z}{H}+u\right)^2}{\sigma^2}\right)\sin\left(-\pi\frac{z}{H}\right), \quad z \in [-H, 0], \tag{2}$$

where $A2$ and u are model coefficients controlling maximum inferior medial bulging $A_{\max,i}$ and the vertical location $z_{\max,i}$ at which the maximum inferior bulging occurs, respectively, and α_i is a scale factor that ranges between 0 and 1. The parameter σ controls the vertical extent of the inferior-medial bulging.

For larynx L1, the location ($z_{\max,s} = 0.27$) and the maximum amplitude ($A_{\max,s} = 0.074$) of the superior-medial bulging were obtained from curve fitting the MRI data [Fig. 1(c)]. For inferior-medial bulging, the parameter $z_{\max,i}$ was set to 0.6 based on the data in Vahabzadeh-Hagh *et al.* (2017), and ($A_{\max,i}$, σ) were set to 0.271 and 0.24, respectively, so that combined superior and inferior bulging at the level of ($\alpha_s = 0.5$,$\alpha_i = 0.5$) produced a rectangular medial surface contour at the midline as in Fig. 1(d). For the convenience of direct comparison between the two larynges, the same control parameters were used in larynx L2.

Figure 4 shows the coronal cross-sectional contours of the two larynges under different conditions of superior and inferior medial bulging. Different combinations of superior- and inferior-medial bulging were able to produce medial surface contours that are similar to those observed in Vahabzadeh-Hagh *et al.* (2017). For example, the curves (α_s,α_i) = (1,0) and (α_s,α_i) = (0,1) are similar to the contours observed under individual LCA and TA muscle activation, respectively, in Vahabzadeh-Hagh *et al.* (2017). Combined superior-medial bulging and inferior-medial bulging with (α_s,α_i) = (0.6,0.6) led to an approximately rectangular glottal configuration, similar to that observed under combined LCA-TA activation in Vahabzadeh-Hagh *et al.* (2017). Note that, although the same parameters of medial bulging control were used for the two larynges, the resulting medial surface contours were still notably different between the two larynges due to differences in their resting medial surface shape and overall dimensions.

C. Voice production simulation procedure and conditions

Voice production simulations were performed for the two larynges as described in Zhang (2015, 2017). Briefly, the vocal fold was modeled as a transversely isotropic, nearly incompressible, linear elastic material with the plane of isotropy perpendicular to the AP direction. The three-dimensional vocal fold model with varying medial surface shape was implemented in finite-element software COMSOL (Comsol Inc., Burlington, MA) as shown in Fig. 3. Although a two-layer vocal fold was modeled, for simplicity identical mechanical properties were used for both layers with the transverse Young's modulus $E_t = 1$ kPa, AP shear modulus $G_{ap} = 20$ kPa, AP Young's modulus $E_{ap} = 80$ kPa, AP Poisson's ratio $\nu_{ap} = 0.495$, and vocal fold density $\rho = 1030\,\text{kg/m}^3$. A fixed boundary condition was applied to the lateral surface and the posterior-medial surface that was in contact with the arytenoid cartilage (Fig. 2). The

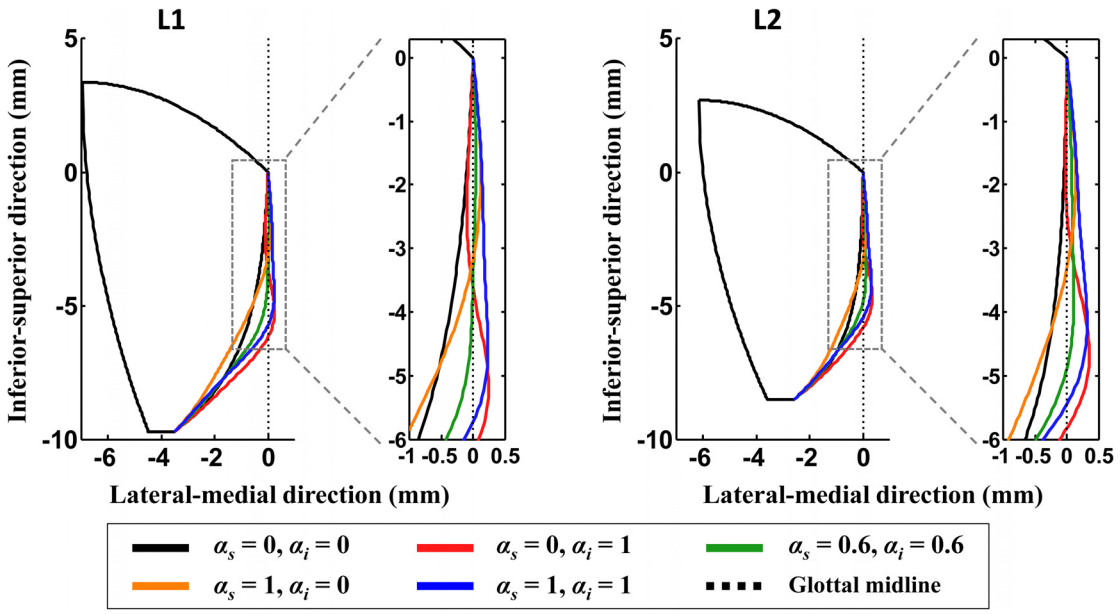

FIG. 4. (Color online) Coronal contours of mid-membranous cross sections (black lines in Fig. 2) of larynges L1 and L2 under five typical conditions of superior and inferior medial bulging. In each panel, the right graph shows a magnified view of the medial surface.

glottal flow was modeled by a one-dimensional quasi-steady flow equation taking into consideration a viscous loss in the airflow. For details of the model, the reader is referred to Zhang (2015, 2017). Our previous studies have shown that the model was able to reproduce observations in physical model experiments (e.g., Zhang and Luu, 2012; Farahani and Zhang, 2016). Model validation against human larynx experiments, however, has to wait until such experimental data (i.e., geometry and mechanical properties of the larynx as well as vibration and acoustics data) become available.

Simulations were performed for different conditions of medial bulging and the subglottal pressure. Six levels each (0, 0.2, 0.4, 0.6, 0.8, and 1) were considered for superior-medial bulging and inferior-medial bulging, leading to 36 medial surface shapes for each larynx. While the medial surface shape often covaries with the degree of vocal fold approximation, in this study the degree of vocal fold approximation was kept constant while the medial surface shape was manipulated in order to focus on the effect of changes in medial surface shape. Specifically, the superior medial edge of the vocal fold was set to align with the glottal midline, i.e., the prephonatory glottal opening was set to zero. For each medial surface condition, the subglottal pressure was varied in a range from 100 to 2400 Pa as in Zhang (2016b, 2017). A total of 1224 conditions were investigated, each simulating a 0.5-s voice production at a sampling rate of 44 100 Hz.

D. Data analysis

For each condition, the last 0.25 s of the simulation, by which time vocal fold vibration generally reached steady state or damped out, was used for analysis. While a series of data analysis was performed, this study focused on the phonation threshold pressure and the closed quotient (CQ) of vocal fold vibration. Phonation threshold pressure was calculated as the lowest subglottal pressure that produced sustained vocal fold vibration for each medial surface condition. The CQ of the glottal flow waveform was calculated as the ratio between the duration of closed phase and the period of the glottal cycle with the closed phase defined as the duration with a glottal flow falls within the lowest ten percent of the glottal flow waveform.

III. RESULTS

A. Effects of medial surface shape

Figure 5 shows the glottal flow waveforms of larynx L1 for the five typical conditions of superior and inferior medial bulging shown in Fig. 4. For the resting medial surface shape (i.e., no superior or inferior medial bulging) and a subglottal pressure of 1.4 kPa, no phonation was observed, and the vocal folds were pushed open with a mean glottal flow rate of 200 ml/s. Sustained vocal fold vibration at the same subglottal pressure was observed with either superior or inferior medial bulging. In comparison, inferior medial bulging led to vibration with a smaller mean flow rate and a slightly higher CQ. With combined superior and inferior medial bulging (each at 0.6), the vocal fold exhibited a subharmonic vibration pattern with a high peak followed by a low peak in the glottal flow waveform. Combined superior and inferior medial bulging at the maximum level (i.e., both at 1) led to a very tight constriction, which completely closed the glottis and exhibited no vibration.

Figure 6 shows the phonation threshold pressure at different conditions of superior and inferior medial bulging for larynx L1. In general, the phonation threshold pressure decreased with an increase in either superior- or inferior-medial bulging at low levels (less than 0.6). However, for very high levels of combined superior- and inferior-medial bulging, the phonation threshold pressure increased rapidly, and no phonation was observed for the highest level of

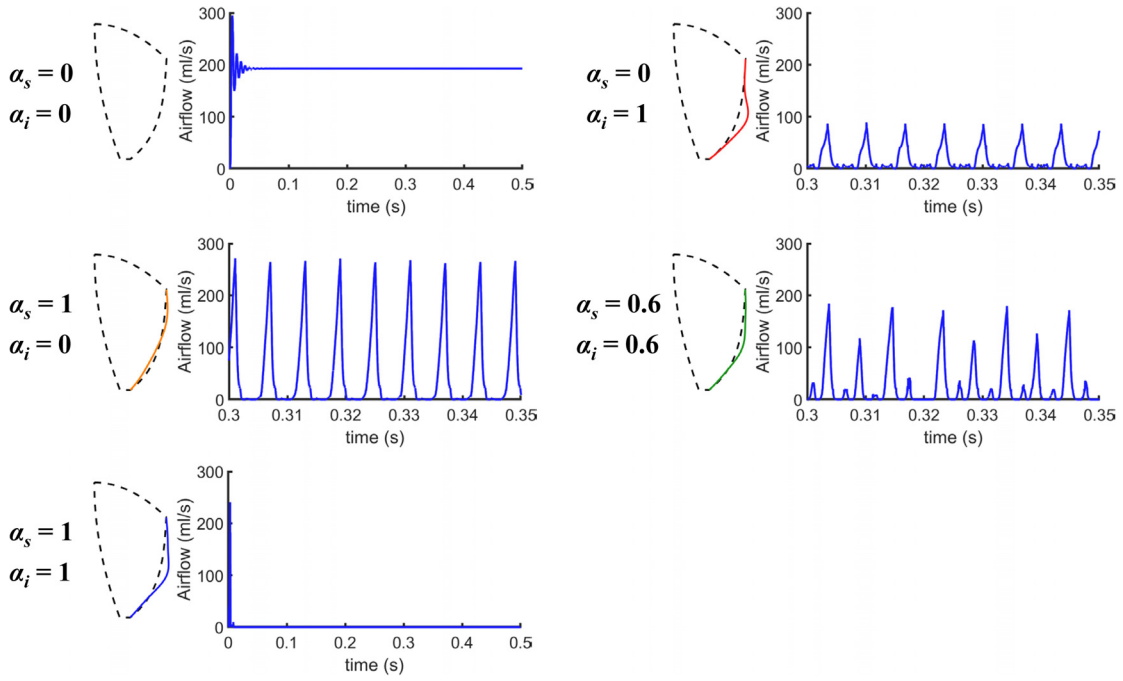

FIG. 5. (Color online) Glottal flow waveforms of larynx L1 at the five typical conditions of superior and inferior medial bulging shown in Fig. 4. The dashed lines and solid lines in the coronal contours represent the medial surface contour at rest and at the corresponding bulging condition, respectively.

combined superior- and inferior-medial bulging in the subglottal pressure range investigated in this study (up to 2.4 kPa).

Figure 6 also shows the CQ as a function of superior- and inferior-medial bulging. In general, the CQ increased with an increase in either the superior- or inferior-medial bulging. Note that the CQ ranges from 0.1 to 0.9 in Fig. 6, indicating a large impact of changes in medial surface shape on the closure pattern of vocal fold vibration.

As shown in Fig. 4, an increase in either superior or inferior medial bulging in this study led to a more rectangular medial surface with an increased effective vertical thickness. Thus, these observations appear to confirm the findings in Zhang (2016b, 2018) regarding the effect of varying medial surface vertical thickness on the glottal flow waveform, phonation threshold pressure, and CQ.

B. Effects of subject-specific anatomical differences

Figure 7 shows the effect of the medial surface shape on the phonation threshold pressure and CQ in larynx L2. The trend was generally similar to that in L1. However, notable differences can be observed. First, the range of variation in the CQ was smaller in L2 than in L1, indicating a weaker effect of medial surface manipulation in L2. Also, at high levels of medial bulging, the phonation threshold pressure remained low in L2, in contrast to the rapidly increasing phonation threshold pressure in L1. Second, superior medial bulging had a much smaller effect in L2 than in L1 on both the phonation threshold pressure and the CQ.

Since the same two-step control parameters were used in both larynges, these differences were likely due to the differences in the individual laryngeal anatomy. In addition to the difference in the overall length, Figs. 2 and 4 show major

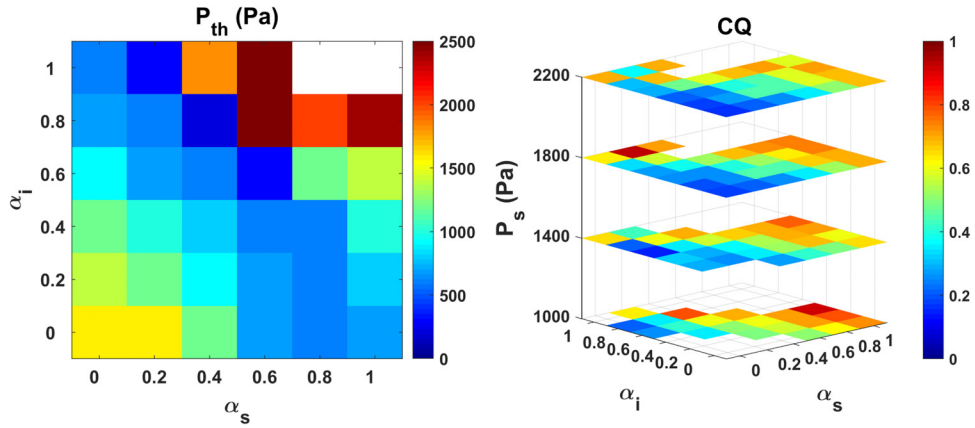

FIG. 6. (Color online) Larynx L1. (Left) phonation threshold pressure (P_{th}) as a function of the superior- and inferior-medial bulging. (Right) CQ as a function of medial bulging and the subglottal pressure (P_s). Regions without data indicate conditions of no phonation.

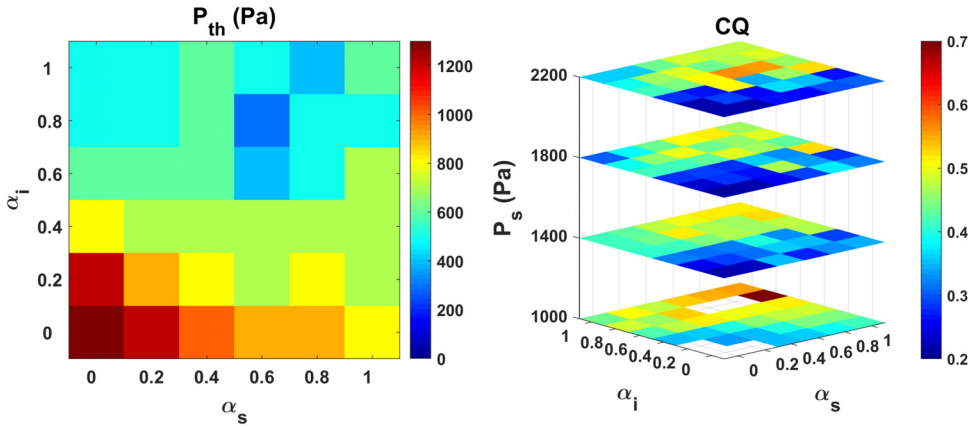

FIG. 7. (Color online) Larynx L2. (Left) Phonation threshold pressure (P_{th}) as a function of the superior- and inferior-medial bulging. (Right) CQ as a function of medial bulging and the subglottal pressure (P_s). Regions without data indicate conditions of no phonation.

differences between the two larynges in the resting medial surface contour and its variation along the AP direction. Specifically, the medial surface of L1 spanned a larger vertical dimension and had a relatively less variation along the AP direction than the medial surface of L2. The superior portion of the medial surface in L2 was also more straight and closer to a rectangular shape than that in L1.

To investigate the potential effects of medial surface dimension and its variation along the AP direction, we created two additional vocal fold models (labeled S1 and S2) by selecting two coronal sections of L2 (marked by black solid line for S1 and blue dashed line for S2 in Fig. 2) and extruding them along the AP direction. The two new models had the same AP length as that of the membranous vocal fold of L2, but had a uniform cross-sectional geometry without variations along the AP direction. As shown in Fig. 2, model S1 was thicker along the vertical direction but narrower along the medial-lateral direction. The medial surface contours in these two models were then manipulated in the same way as in the L2 model, and the resulting voice production was compared to L2. We hypothesized that if the medial surface dimension or its variation along the AP direction had a large impact on voice production, we would observe a significant difference in voice production between S1 and S2 and between both section models and the L2 model.

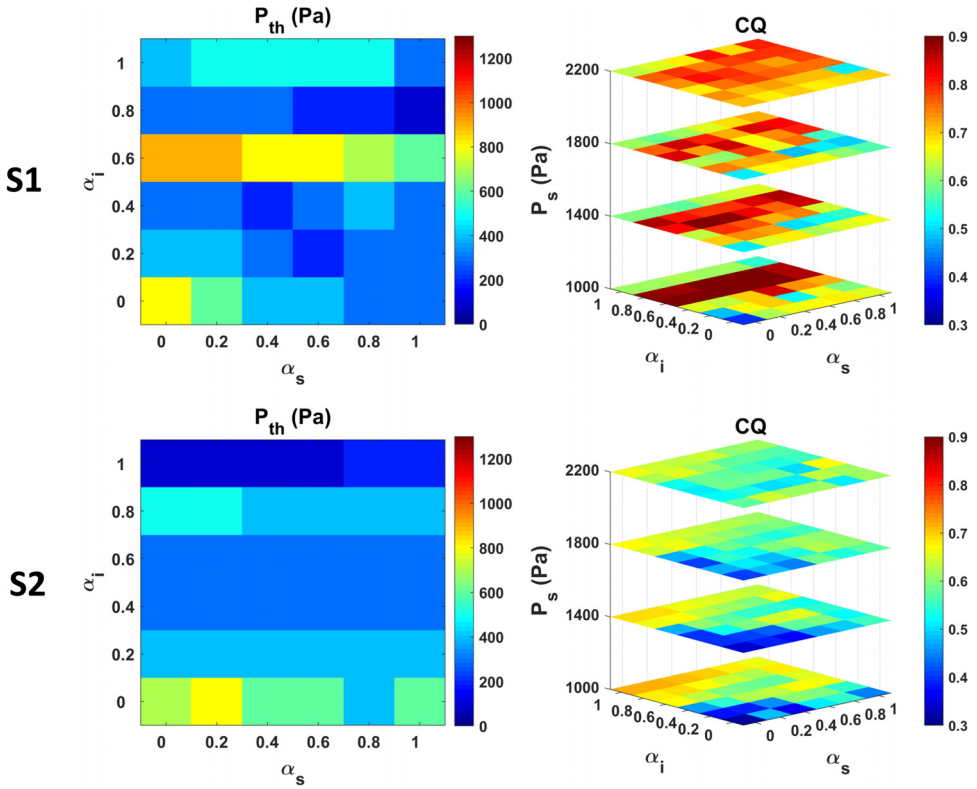

FIG. 8. (Color online) Results for the two section models S1 (top) and S2 (bottom) derived from larynx L2. Left: phonation threshold pressure (P_{th}) as a function of the superior- and inferior-medial bulging. Right: CQ as a function of medial bulging and the subglottal pressure (P_s).

Figure 8 shows phonation threshold pressure and CQ at different conditions for the two section models S1 and S2. Both models had lower phonation threshold pressures than those in L2, especially at low levels of medial bulging. The CQ in S1 was significantly higher than that in S2, which was comparable to that in L2. The difference between S1 and S2 showed that cross-sectional geometry had an important effect on voice production, whereas the difference between the two section models and L2 showed that the AP variation of cross-sectional geometry also mattered. These differences may be explained by, among other factors, the differences in the effective vertical thickness among the models. The S1 model was the thickest among the three, which may have contributed to the generally higher values of the CQ. With variation in vertical thickness along the AP direction, the CQ in L2 would likely be determined by the thinnest cross sections, which may explain the similar range of CQ in S2 and L2.

Note that in all three models (S1, S2, and L2), the superior medial bulging had a smaller effect on the phonation threshold pressure than the inferior medial bulging. This was probably because the superior portion of the medial surface in all three models was already quite straight and closer to a rectangular shape than that in L1 (Fig. 4), which may have reduced the influence of any further superior medial bulging.

Figure 8 shows that in model S1, the phonation threshold pressure became notably high at conditions of $\alpha_i = 0.6$. Examination of the data revealed that this increase in phonation threshold pressure was due to a transition between different vocal fold vibration modes, similar to that described in Zhang (2018).

IV. DISCUSSION AND CONCLUSIONS

In this study, using a larynx-specific vocal fold model based on three-dimensional MRI images of excised human larynges, we showed that manipulation of the medial surface shape, as occurs in human vocal fold posturing, could have a significant effect on the phonation threshold pressure and closure pattern of vocal fold vibration. Specifically, an increase in either superior or inferior medial bulging significantly lowered the phonation threshold pressure and increased the CQ. In larynx L1, we also observed that the phonation threshold pressure started to increase rapidly, and vocal fold vibration became irregular at very high levels of combined superior and inferior medial bulging.

The results are generally consistent with previous studies using simplified vocal fold geometry. It has been shown in earlier studies that vocal folds with a rectangular or nearly rectangular medial surface have the lowest phonation threshold pressure, and the phonation threshold pressure increases significantly for either a convergent or divergent medial surface (Chan *et al.*, 1997; Lucero, 1998; Zhang, 2008). Increasing inferior medial bulging tends to reduce the vibration amplitude and mean glottal flow (Titze and Talkin, 1979; Alipour and Scherer, 2000). Changes in vertical thickness have been shown to have a large effect on both the phonation threshold pressure (Zhang, 2017) and the CQ of vocal fold vibration (Zhang, 2016b, 2017). In some sense, these two features, vertical thickness and medial surface convergence, appear to be related in models based on realistic vocal fold geometry. Medial bulging, particularly inferior medial bulging, changes the medial surface from convergent to rectangular, which also effectively increases the vertical thickness of the medial surface.

One original motivation of this study was to explore the possibility of defining an effective vertical thickness measure for any given medial surface contour so that it can be used to predict and compare the CQ across different larynges. Our initial effort showed that when an effective thickness was defined as the vertical span of the portion of the medial surface that falls within a threshold distance of the glottal midline, similar to Hampala *et al.* (2015), it was able to collapse the CQ data as a function of the effective thickness, with much reduced data scattering when a smaller threshold distance (0.05 mm or smaller) was used. Figure 9 shows an example of this for an effective thickness calculated at the mid-membranous cross section. Note that all vocal fold conditions in our study were fully approximated. For non-fully approximated conditions, a different definition will need to be used. However, this effective thickness definition was not able to collapse data from the two larynges. It appears that calculation of an effective thickness for CQ prediction would need to take into consideration the variation of medial surface shape along both the vertical and AP directions, which will be further attempted in the future.

Note that significant changes in the phonation threshold pressure and CQ were observed in this study despite that the degree of vocal fold approximation was kept constant. This suggests that although vocal fold approximation is often considered important to achieving a low phonation threshold pressure and glottal closure during phonation, the medial

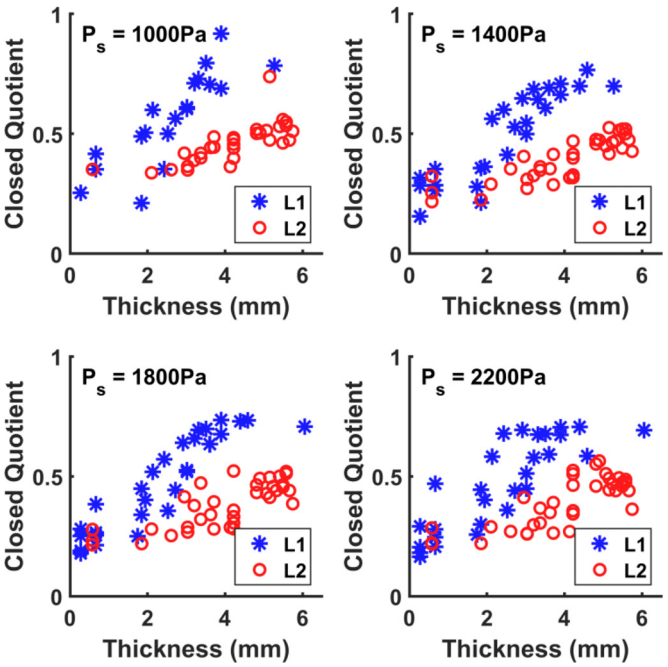

FIG. 9. (Color online) CQ of larynx L1 (asterisk) and L2 (circle) as a function of the effective medial surface thickness for different subglottal pressures (P_s).

surface shape is at least as important as vocal fold approximation and should receive more attention. In particular, clinical intervention (e.g., medialization laryngoplasty or injection augmentation) of glottal insufficiency currently often focuses on reducing the glottal gap as visualized from above. Our results showed that these surgical interventions should also aim to achieve or restore a rectangular and sufficiently thick medial surface, such as the green lines in Fig. 4. A convergent medial surface would lead to a short duration of glottal closure, whereas an overly thick medial surface may require a very high subglottal pressure to phonate, and the resulting voice is often irregular.

Another important contribution of this study was toward identifying laryngeal properties that may contribute to intersubject variability in voice production. Such variability is widely observed in excised larynx experiments, in which seemingly identical aerodynamic and posturing conditions would lead to different voice production in different larynges. This study showed that differences in cross-sectional geometry and its variation along the AP direction can contribute to this variability, and thus need to be taken into consideration, particularly in clinical intervention of voice disorders in which accurate prediction of voice outcome is desired.

In this study, the maximum degrees of superior and inferior medial bulging were determined by empirically curve fitting the model to previous experimental studies. In humans, the maximum medial bulging possible would vary across subjects, laryngeal muscle conditioning, and laryngeal anatomy. Due to the sensitivity of voice production to changes in medial surface shape as demonstrated in this study, it is reasonable to expect slightly different results for different settings of maximum medial bulging. Also, in order to isolate the effects of changes in medial surface shape on voice production, in this study the vocal folds were fully approximated while the medial surface shape was manipulated. In humans, medial surface shape is controlled by laryngeal muscle activation, which also simultaneously regulates vocal fold approximation, vocal fold length, and stiffness and tension within the vocal folds. Thus, direct comparison of the results of this study to recent *in vivo* experiments is not possible at the present time. One future goal is to develop a vocal fold posturing model that integrates all these posture changes through either directly modeling laryngeal muscle activation or developing empirical rules based on recent human and animal experiments.

ACKNOWLEDGMENTS

This study was supported by research Grant Nos. R01DC009229 and R01DC001797 from the National Institute on Deafness and Other Communication Disorders, the National Institutes of Health.

Alipour, F., and Scherer, R. C. (**2000**). "Vocal fold bulging effects on phonation using a biophysical computer model," J. Voice **14**(4), 470–483.

Berry, D. A., Montequin, D. W., and Tayama, N. (**2001**). "High-speed digital imaging of the medial surface of the vocal folds," J. Acoust. Soc. Am. **110**(5), 2539–2547.

Chan, R. W., Titze, I. R., and Titze, M. R. (**1997**). "Further studies of phonation threshold pressure in a physical model of the vocal fold mucosa," J. Acoust. Soc. Am. **101**(6), 3722–3727.

Chhetri, D. K., Neubauer, J., and Berry, D. A. (**2012**). "Neuromuscular control of fundamental frequency and glottal posture at phonation onset," J. Acoust. Soc. Am. **131**(2), 1401–1412.

Chhetri, D. K., Neubauer, J., Sofer, E., and Berry, D. A. (**2014**). "Influence and interactions of laryngeal adductors and cricothyroid muscles on fundamental frequency and glottal posture control," J. Acoust. Soc. Am. **135**(4), 2052–2064.

Döllinger, M., Berry, D. A., and Berke, G. S. (**2005**). "Medial surface dynamics of an *in vivo* canine vocal fold during phonation," J. Acoust. Soc. Am. **117**(5), 3174–3183.

Farahani, M., and Zhang, Z. (**2016**). "Experimental validation of a three-dimensional reduced-order continuum model of phonation," J. Acoust. Soc. Am. **140**(2), EL172–EL177.

Hampala, V., Laukkanen, A., Guzman, M. A., Horáček, J., and Švec, J. G. (**2015**). "Vocal fold adjustment caused by phonation into a tube: A double-case study using computed tomography," J. Voice **29**(6), 733–742.

Hirano, M. (**1988**). "Vocal mechanisms in singing: Laryngological and phoniatric aspects," J. Voice **2**(1), 51–69.

Lucero, J. C. (**1998**). "Optimal glottal configuration for ease of phonation," J. Voice **12**(2), 151–158.

Mau, T., Muhlestein, J., Callahan, S., and Chan, R. W. (**2012**). "Modulating phonation through alteration of vocal fold medial surface contour," Laryngoscope **122**(9), 2005–2014.

Pickup, B. A., and Thomson, S. L. (**2011**). "Identification of geometric parameters influencing the flow-induced vibration of a two-layer self-oscillating computational vocal fold model," J. Acoust. Soc. Am. **129**(4), 2121–2132.

Scherer, R. C., Shinwari, D., De Witt, K., Zhang, C., Kucinschi, B. R., and Afjeh, A. A. (**2001**). "Intraglottal pressure profiles for a symmetric and oblique glottis with a divergence angle of 10 degrees," J. Acoust. Soc. Am. **109**(4), 1616–1630.

Sundberg, J., and Högset, C. (**2001**). "Voice source differences between falsetto and modal registers in counter tenors, tenors and baritones," Logoped. Phoniatr. Vocol. **26**(1), 26–36.

Thomson, S. L., Mongeau, L., and Frankel, S. H. (**2005**). "Aerodynamic transfer of energy to the vocal folds," J. Acoust. Soc. Am. **118**(3), 1689–1700.

Titze, I. R., and Talkin, D. T. (**1979**). "A theoretical study of the effects of various laryngeal configurations on the acoustics of phonation," J. Acoust. Soc. Am. **66**(1), 60–74.

Vahabzadeh-Hagh, A. M., Zhang, Z., and Chhetri, D. K. (**2017**). "Quantitative evaluation of the *in vivo* vocal fold medial surface shape," J. Voice **31**(4), 513.e15–513.e23.

Wu, L., and Zhang, Z. (**2016**). "A parametric vocal fold model based on magnetic resonance imaging," J. Acoust. Soc. Am. **140**(2), EL159–EL165.

Yin, J., and Zhang, Z. (**2016**). "Laryngeal muscular control of vocal fold posturing: Numerical modeling and experimental validation," J. Acoust. Soc. Am. **140**(3), EL280–EL284.

Zhang, Z. (**2008**). "Influence of flow separation location on phonation onset," J. Acoust. Soc. Am. **124**(3), 1689–1694.

Zhang, Z. (**2015**). "Regulation of glottal closure and airflow in a three-dimensional phonation model: Implications for vocal intensity control," J. Acoust. Soc. Am. **137**, 898–910.

Zhang, Z. (**2016a**). "Mechanics of human voice production and control," J. Acoust. Soc. Am. **140**(4), 2614–2635.

Zhang, Z. (**2016b**). "Cause-effect relationship between vocal fold physiology and voice production in a three-dimensional phonation model," J. Acoust. Soc. Am. **139**(4), 1493–1507.

Zhang, Z. (**2017**). "Effect of vocal fold stiffness on voice production in a three-dimensional body-cover phonation model," J. Acoust. Soc. Am. **142**(4), 2311–2321.

Zhang, Z. (**2018**). "Vocal instabilities in a three-dimensional body-cover phonation model," J. Acoust. Soc. Am. **144**(3), 1216–1230.

Zhang, Z., and Luu, T. (**2012**). "Asymmetric vibration in a two-layer vocal fold model with left-right stiffness asymmetry: Experiment and simulation," J. Acoust. Soc. Am. **132**(3), 1626–1635.